Title

The fibrin-derived gamma377-395 peptide inhibits microglia activation and suppresses relapsing paralysis in central nervous system autoimmune disease.

Journal

The Journal of experimental medicine, 204(3)

ISSN

0022-1007

Authors

Adams, Ryan A
Bauer, Jan
Flick, Matthew J
et al.

Publication Date

2007-03-01

DOI

10.1084/jem.20061931

Peer reviewed

The fibrin-derived $\gamma^{377-395}$ peptide inhibits microglia activation and suppresses relapsing paralysis in central nervous system autoimmune disease

Ryan A. Adams,[1] Jan Bauer,[2] Matthew J. Flick,[3] Shoana L. Sikorski,[1] Tal Nuriel,[1] Hans Lassmann,[2] Jay L. Degen,[3] and Katerina Akassoglou[1]

[1]Department of Pharmacology, University of California, San Diego, La Jolla, CA 92093
[2]Center for Brain Research, Medical University of Vienna, A-1090 Vienna, Austria
[3]Children's Hospital Research Foundation and the University of Cincinnati College of Medicine, Cincinnati, OH 45229

Perivascular microglia activation is a hallmark of inflammatory demyelination in multiple sclerosis (MS), but the mechanisms underlying microglia activation and specific strategies to attenuate their activation remain elusive. Here, we identify fibrinogen as a novel regulator of microglia activation and show that targeting of the interaction of fibrinogen with the microglia integrin receptor Mac-1 ($\alpha_M\beta_2$, CD11b/CD18) is sufficient to suppress experimental autoimmune encephalomyelitis in mice that retain full coagulation function. We show that fibrinogen, which is deposited perivascularly in MS plaques, signals through Mac-1 and induces the differentiation of microglia to phagocytes via activation of Akt and Rho. Genetic disruption of fibrinogen–Mac-1 interaction in fibrinogen-$\gamma^{390-396A}$ knock-in mice or pharmacologically impeding fibrinogen–Mac-1 interaction through intranasal delivery of a fibrinogen-derived inhibitory peptide ($\gamma^{377-395}$) attenuates microglia activation and suppresses relapsing paralysis. Because blocking fibrinogen–Mac-1 interactions affects the proinflammatory but not the procoagulant properties of fibrinogen, targeting the $\gamma^{377-395}$ fibrinogen epitope could represent a potential therapeutic strategy for MS and other neuroinflammatory diseases associated with blood-brain barrier disruption and microglia activation.

CORRESPONDENCE
Katerina Akassoglou:
akass@ucsd.edu

Abbreviations used: BBB, blood-brain barrier; CNS, central nervous system; EAE, experimental autoimmune encephalomyelitis; iNOS, inducible nitric oxide synthase; MOG, myelin oligodendrocyte glycoprotein; MS, multiple sclerosis; PI3K, phosphoinositide 3-kinase; PLP, proteolipid protein; TLR, Toll-like receptor.

Multiple sclerosis (MS) is a chronic inflammatory demyelinating disease of the nervous system in which an inflammatory process is associated with destruction of myelin sheaths and later with axonal damage leading to permanent functional deficits, such as paralysis and loss of vision (1). Resident microglia are considered responsible for the effector mechanism leading to demyelination via their ability to phagocytose myelin and secrete proinflammatory cytokines (2). Microglia are necessary not only for the maintenance but also for the onset of inflammatory demyelination in central nervous system (CNS) autoimmune disease (3), suggesting that attenuation of the microglia response could represent a promising therapeutic target for MS (2). Although microglia represent a potentially powerful target for therapeutic intervention (4), the mechanisms of perivascular microglia activation in inflammatory demyelination as well as a strategy to limit their activation in MS have not been identified.

In MS lesions, perivascular activation of microglia colocalizes with areas of blood-brain barrier (BBB) disruption (5). Magnetic resonance imaging studies link BBB breakdown with clinical relapse (6). Moreover, in vivo live imaging showed that BBB disruption provokes the immediate and focal activation of microglia (7). However, the molecular mechanism that links BBB disruption with microglia activation and disease pathogenesis remains elusive. One of the earliest events coupled to BBB disruption in MS is leakage of the blood protein fibrinogen in the nervous system that results in perivascular deposition of fibrin (8–11). Although fibrinogen has been primarily studied for its functions

T. Nuriel's present address is Weill Medical School of Cornell University, New York, NY 10021.
The online version of this article contains supplemental material.

in blood coagulation, there is appreciable evidence that fibrinogen plays a pivotal role in the inflammatory response (12, 13) and host defense (14, 15). Fibrinogen is a classic acute-phase reactant, characterized by a unique molecular structure with binding sites for cellular receptors that regulate the inflammatory process (16, 17). Research in MS animal models shows that prophylactic fibrin depletion either by genetic depletion of fibrinogen (18) or by prophylactic administration of anti-coagulants (18, 19) ameliorates disease pathogenesis. Although these studies show that prophylactic depletion of fibrin could be beneficial in MS, the use of anti-coagulants would potentially have limited therapeutic value due to the hemorrhagic side effects after prolonged use of fibrin-depleting agents.

We sought to design a therapeutic strategy that would block the damaging effects of fibrinogen in the nervous system without affecting its beneficial effects in blood coagulation by identifying and targeting the fibrinogen receptor in the nervous system. Impeding the interaction of fibrinogen with selected integrin receptors has been previously used as a strategy for drug development. Disruption of fibrinogen interaction with the platelet integrin receptor $\alpha_{IIb}\beta_3$ using either small molecule inhibitors or antibodies (e.g., ReoPro, abciximab) is highly effective at limiting thrombotic events in patients with vessel wall disease (20). We hypothesized that if we identified the specific cell type in the CNS responsive to fibrinogen and established the specific fibrinogen receptor used by these cells, we may be able to block the deleterious cellular responses associated with fibrin deposition in the nervous system without affecting its beneficial coagulant properties.

Recent evidence showed that paralysis of $CD11b^+$ microglia ameliorates inflammatory demyelination in the presence of peripheral T cells and macrophages (3). CD11b is the α chain of the integrin receptor Mac-1 ($\alpha_M\beta_2$, CD11b/CD18) that in inflammatory demyelination regulates phagocytosis of myelin (21, 22). Myelin phagocytosis is thought to be subjected to modulation between inactive and active states of Mac-1 (23). Immobilized fibrinogen and insoluble fibrin, but not soluble fibrinogen, have been identified as physiological, high-affinity ligands for Mac-1 (15, 24, 25). Interestingly, in MS lesions fibrin deposition colocalizes with areas of activated microglia (11). Here, we show that fibrinogen controls differentiation of microglia to phagocytes via the integrin receptor Mac-1. Moreover, a fibrinogen-derived peptide known to inhibit Mac-1 ($\gamma^{377-395}$ peptide) blocks microglia activation in vitro. Importantly, complementary in vivo studies using either the inhibitory $\gamma^{377-395}$ peptide or mice expressing a mutant form of fibrinogen lacking the Mac-1 binding motif establish that targeting the fibrin–Mac-1 interaction is a novel and potentially effective therapeutic strategy for inflammatory demyelination. These studies show for the first time that fibrin induces microglia activation and that targeting the inflammatory but not the procoagulant properties of fibrinogen is sufficient to suppress microglia activation and inflammatory demyelinating disease.

RESULTS

Fibrinogen directly activates microglia resulting in cytoskeletal rearrangements and increased phagocytosis

We first tested the effects of fibrinogen on pure primary microglia cells. Immobilized fibrinogen had a dramatic effect on microglia activation characterized by an increase in cell size (Fig. 1 A, top right) when compared with untreated controls (Fig. 1 A, top left). Quantitation revealed 85.5 ± 1.4% of activated microglia after fibrinogen treatment versus 8.2 ± 3.4% in untreated cells (Fig. 1 B; $P < 0.001$). In contrast to immobilized fibrinogen, soluble fibrinogen did not induce changes in microglia morphology (not depicted). LPS was used as a positive control (Fig. 1, A and B). Using an endotoxin determination assay, we verified that there was no LPS contamination in the fibrinogen-treated cultures. To assess the functional effect of this morphologic activation, we performed phagocytosis assays. Fibrinogen stimulation resulted in a 65.3%

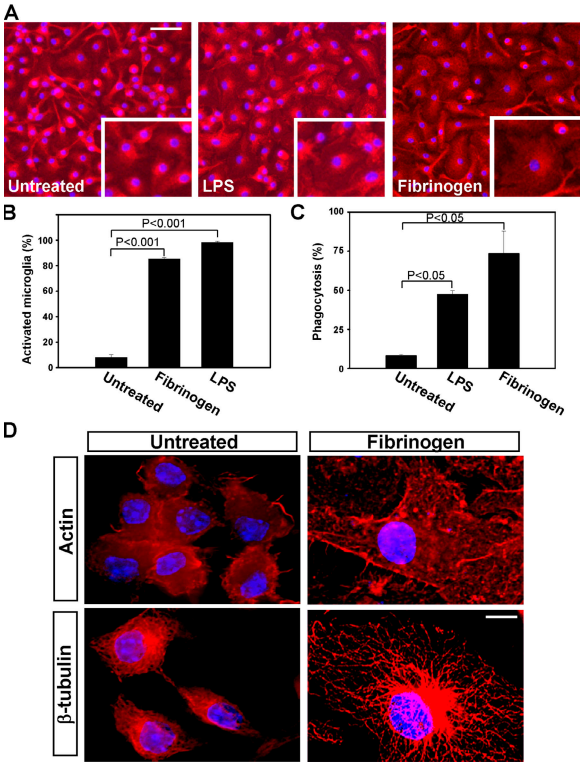

Figure 1. Fibrinogen directly activates microglia resulting in cytoskeletal rearrangements and increased phagocytosis. (A) IsoB4/DAPI immunostained microglia cultured on immobilized fibrinogen have increased cell body size adopting an amoeboid morphology (right). Untreated primary microglia show small cell bodies and thin, bipolar processes (left). LPS-treated cells show activated morphology characterized by cell body swelling (middle). Bar, 26 μm; inset, 21 μm. (B) Quantitation of microglia activation reveals a dramatic increase upon fibrinogen stimulation. (C) Fibrinogen-stimulated microglia showed increased phagocytosis of fluorescent *Escherichia coli* as compared with untreated microglia. LPS served as a positive control. (D) Deconvolution microscopy of primary microglia revealed significant rearrangements of the cytoskeleton upon treatment with fibrinogen. Microglia were stained with antibodies to actin and β-tubulin in red, and the nucleus was stained blue with DAPI. Bar, 4.4 μm.

increase in phagocytosis as compared with untreated controls ($P < 0.05$), whereas LPS incubation, by comparison, increased phagocytosis by 39.1% (Fig. 1 C; $P < 0.05$). Previous studies have demonstrated that dynamic rearrangements of both the actin (26) and microtubule (27) networks are critical for phagocytosis. Deconvolution microscopy showed that fibrinogen stimulation resulted in dramatic rearrangement of the microglial cytoskeleton as determined by immunostaining of actin and β-tubulin (Fig. 1 D). Collectively, these results suggest that fibrinogen induces microglia differentiation into a phagocytic state.

Fibrinogen activates microglia via the Mac-1 integrin receptor

Mac-1 orchestrates the innate immune response by regulating phagocyte adhesion, migration, and engulfment of complement-opsonized particles (28). M1/70, an antibody that blocks binding of fibrinogen to CD11b (24, 29), inhibited fibrinogen-mediated microglia activation (Fig. 2 A). Quantitation showed 71 ± 4.9% of activated microglia in fibrinogen-treated cells versus 18 ± 0.7% in cells treated with fibrinogen in the presence of M1/70 (Fig. 2 B; $P < 0.01$). The inhibitory effect of M1/70 was specific for fibrinogen and did not affect LPS-mediated activation of microglia (Fig. 2 B). Moreover, blocking CD11b reduced phagocytosis of fibrinogen-treated cells by 40% (Fig. 2 C; $P < 0.05$). Previous studies have established that the Toll-like receptor (TLR)4 LPS receptor mediates LPS-induced microglia activation (30, 31). In contrast, blocking TLR-4 did not affect fibrinogen-mediated phagocytosis, suggesting that Mac-1 was the major receptor to induce fibrinogen-mediated phagocytosis (Fig. 2 C).

RhoA and phosphoinositide 3-kinase (PI3K) are the two major signaling pathways downstream of Mac-1 that mediate the cytoskeletal rearrangements for the induction of phagocytosis (28, 32, 33). Fibrinogen induced a 1.9-fold increase of active RhoA and a 24-fold increase in Akt phosphorylation in microglia (Fig. 2 D). Furthermore, blocking the PI3K signaling pathway using LY294002 inhibited the fibrinogen-induced increase of phagocytosis in microglia (Fig. 2 C; $P < 0.01$), suggesting that PI3K is downstream of fibrinogen–Mac-1 signaling in microglia cells. This is the first evidence suggesting that fibrinogen can induce Mac-1–dependent signaling in microglia.

Analysis of demyelinated spinal cords after the induction of proteolipid protein $(PLP)_{139-151}$ experimental autoimmune encephalomyelitis (EAE) in mice showed that $CD11b^+$ microglia (Fig. 2 E, green) were surrounded by fibrin (Fig. 2 E, red). Similarly, analysis of acute demyelinating lesions of human MS showed that fibrin (Fig. 2 F, green) surrounded activated microglia cells (Fig. 2 F, red). Collectively, these results show that fibrinogen/CD11b signaling induces phagocytosis in microglia and demonstrate both in EAE and in human MS

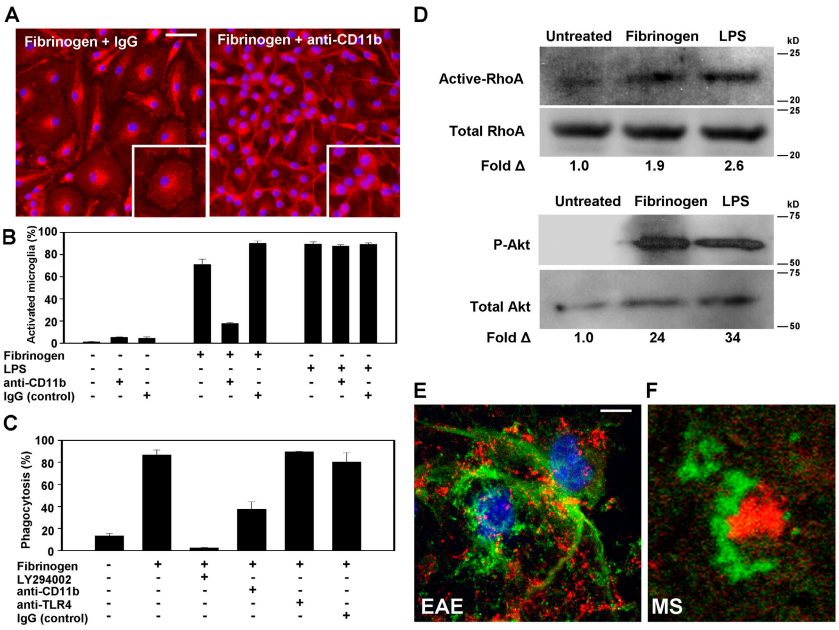

Figure 2. Fibrinogen directly activates microglia via the Mac-1 integrin receptor. (A) Fibrinogen-induced morphologic activation of microglia is blocked by the addition of a rat anti-CD11b neutralizing antibody (M1/70). Rat IgG (control) did not change the effects of fibrinogen in microglia activation. Bar, 39 μm; inset, 17 μm. (B) Quantitation of microglia activation reveals that the Mac-1 neutralizing antibody blocks fibrinogen-induced activation but not LPS activation of microglia. (C) Increased microglia phagocytosis upon fibrinogen stimulation is blocked by the addition of a PI3K inhibitor (LY294002) and diminished in the presence of a CD11b neutralizing antibody. A control anti-TLR4 or IgG showed no reduction in fibrinogen-stimulated phagocytosis. (D) Western blots show increased active RhoA and Akt activation upon fibrinogen stimulation of microglia. In both assays, LPS served as a positive control. (E) Confocal microscopy demonstrates the spatial interaction between $CD11b^+$ cells (green) and fibrin (red) in spinal cords from $PLP_{139-151}$–immunized mice. (F) Confocal double immunofluorescence shows fibrin (green) surrounding an activated microglia (red) in a human early demyelinating plaque of acute MS. Bars: E, 6.7 μm; F, 15 μm.

the presence of this ligand–receptor system on active microglia within inflammatory demyelinating lesions.

Fibrin depletion inhibits microglia activation in vivo and attenuates inflammatory demyelination

We further examined whether fibrin is required for the activation of Mac-1$^+$ cells in vivo. We administered the anti-coagulant ancrod (34) in an established remitting-relapsing model of $PLP_{139-151}$ EAE (35) after the development of the first paralytic incidence. At the time of the first relapse, untreated mice show dramatic activation of CD11b$^+$ cells characterized by thick processes (Fig. 3 A, left, green). In contrast, in ancrod-treated mice, CD11b$^+$ cells appear with ramified morphology (Fig. 3 A, right, green) resembling CD11b$^+$ cells in the normal spinal cord (Fig. S1, available at http://www.jem.org/cgi/content/full/jem.20061931/DC1). Single channel images are shown in Fig. S1. Untreated mice showed extensive inflammatory demyelinating lesions in the cerebellum (Fig. S2, asterisk) and spinal cord (Fig. S2, arrows). In contrast, in ancrod-treated mice, inflammatory demyelination was dramatically decreased (Fig. S2). Ancrod treatment resulted in decreased demyelination by sevenfold in the cerebellum and by twofold in the spinal cord. Splenocytes isolated from untreated and ancrod-treated mice showed no difference in proliferation upon stimulation with $PLP_{139-151}$ (Fig. S3), further suggesting that CD11b$^+$ cells are the major cell target of fibrin in the nervous system. Fibrin-depleted mice recovered faster from the first paralytic incidence and in contrast to control mice never relapsed (Fig. 3 B). In a rotarod behavioral test performed before the first relapse of the untreated group, fibrin-depleted mice showed a threefold increase of motor strength and coordination when compared with the untreated group (Fig. 3 C). Control nonimmunized mice show values of ~500 s on this assay. Collectively, these results suggest that fibrin is a major contributor to the local activation of CD11b$^+$ cells in vivo. In addition, this is the first demonstration that an anti-coagulant may improve clinical symptoms and reduce inflammatory demyelination when administered after the onset of paralytic symptoms.

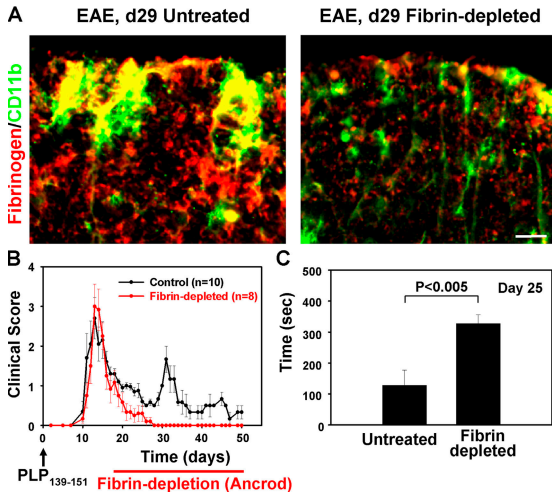

Figure 3. Fibrin depletion using ancrod reverses relapsing paralysis and reduces microglia activation in EAE. (A) Immunofluorescence of control (left) and fibrin-depleted (right) spinal cord with antibodies against fibrinogen (red) and CD11b (green). Activated CD11b$^+$ cells colocalize with fibrin deposition in the control spinal cord (yellow). Bar, 8.4 μm. (B) Clinical scores of $PLP_{139-151}$–immunized mice. Fibrin depletion begins after the first paralytic episode. Fibrin-depleted mice (red circles; $n = 8$) did not develop first or second relapses as compared with control mice (black circles; $n = 10$). (C) Rotarod motor strength and coordination test. Fibrin-depleted mice outperformed immunized control untreated mice on day 25 after immunization. Data are represented as the mean clinical score and are mean ± SEM.

Fib$^{\gamma 390-396A}$ mice have reduced clinical scores and CNS inflammatory lesions

To examine the contribution of fibrinogen–Mac-1 signaling in vivo, we used mice with a knock-in mutation of seven amino acids at residues (N^{390}RLSIGE^{396}) to alanine residues (A^{390}AAAAAA^{396}) that abolishes fibrinogen binding to the Mac-1 receptor (15). These mice, termed *Fib$^{\gamma 390-396A}$*, show decreased Mac-1–mediated neutrophil adhesion resulting in decreased bacterial clearance (15). *Fib$^{\gamma 390-396A}$* and their age- and sex-matched littermate controls (*Fib$^{\gamma WT}$*) were backcrossed six generations to C57BL/6 background (15) and immunized with myelin oligodendrocyte glycoprotein $(MOG)_{35-55}$ peptide (Fig. 4 A). *Fib$^{\gamma 390-396A}$* mice ($n = 29$) showed an average clinical score of 2.1 ± 0.32 (ataxia) at day 20 after immunization, whereas the *Fib$^{\gamma WT}$* mice ($n = 28$) developed clinical symptoms of paralysis, showing an average score of 3.3 ± 0.22 (hind limb paralysis; $P < 0.01$). On day 20, in the *Fib$^{\gamma WT}$* mouse group, 74% of *Fib$^{\gamma WT}$* mice (14/19) were paralyzed, in contrast to 35% of *Fib$^{\gamma 390-396A}$* mice (7/20; clinical score > 3; Fig. 4 B), further demonstrating decreased severity of EAE. *Fib$^{\gamma 390-396A}$* mice showed a 1.5-fold increase in motor skills when compared with *Fib$^{\gamma WT}$* mice (*Fib$^{\gamma 390-396A}$*, 269 ± 9 s vs. *Fib$^{\gamma WT}$*, 169 ± 23 s; $P < 0.05$; Fig. 4 E). Inflammatory lesions were decreased threefold in *Fib$^{\gamma 390-396A}$* mice when compared with *Fib$^{\gamma WT}$* (Fig. 4 C; $P < 0.05$). Demyelination was reduced in *Fib$^{\gamma 390-396A}$* mice (1.57 ± 0.89%) when compared with *Fib$^{\gamma WT}$* (4.17 ± 0.83%; $P < 0.04$). In accordance, spinal cord sections showed a decrease of IsoB4$^+$ cells in *Fib$^{\gamma 390-396A}$* mice when compared with *Fib$^{\gamma WT}$* controls (Fig. 4 F). Decrease in clinical severity was also observed at later time points after the immunization (Fig. 4, A and B). In addition, 25% of *Fib$^{\gamma WT}$* mice (7/28) died compared with only 3% of the *Fib$^{\gamma 390-396A}$* mice (1/29; Fig. 4 D; $P < 0.03$). Collectively, these results suggest that the $\gamma^{390-396}$ binding site of fibrinogen to Mac-1 regulates the severity of EAE.

The fibrin $\gamma^{377-395}$ peptide blocks microglia activation in vitro

Both the in vitro (Fig. 2) and in vivo experiments (Fig. 4) show that fibrinogen signaling through the Mac-1 receptor contributes to microglia activation and regulates the severity of EAE. Biochemical studies identified that the γ^{377}YSMKKTTMKIIPFNRLTIG^{395} peptide blocks fibrin binding to Mac-1 (29). The $\gamma^{377-395}$ is a cryptic epitope in the fibrinogen

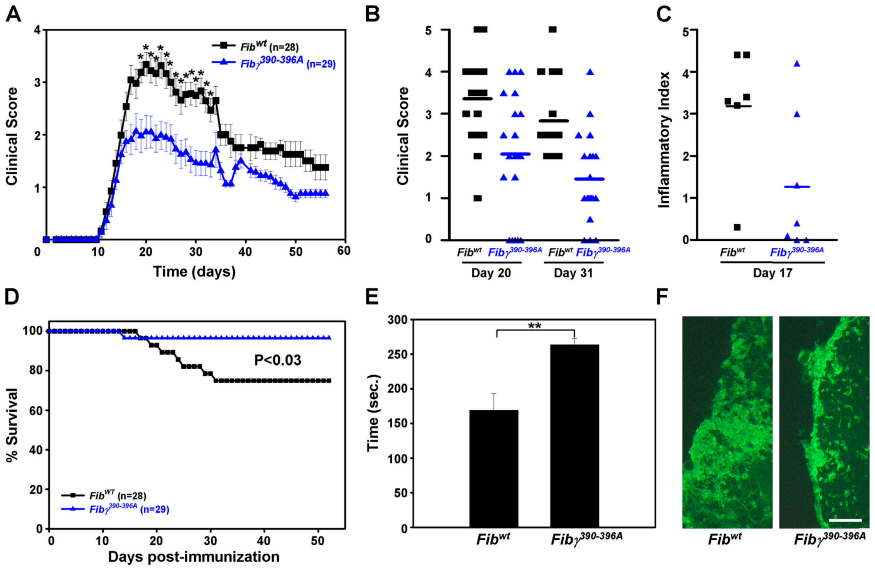

Figure 4. *Fibγ390-396A* mice have reduced clinical scores and microglia activation in EAE. (A) Clinical scores of MOG_{35-55}–immunized mice. *Fibγ390-396A* mice (blue triangles; $n = 29$) show statistically significant lower clinical scores (*, $P < 0.01$) than *FibγWT* control mice (black squares; $n = 28$). (B) Individual clinical scores from *Fibγ390-396A* and *FibγWT* mice on days 20 (average clinical score, 3.3 ± 0.22 for *FibγWT* [$n = 19$] vs. 2.1 ± 0.32 for *Fibγ390-396A* [$n = 20$]; $P < 0.01$) and 31 after immunization (average clinical score, 2.8 ± 0.25 for *FibγWT* [$n = 15$] vs. 1.5 ± 0.23 for *Fibγ390-396A* [$n = 20$]; $P < 0.001$). (C) Histological analysis of spinal cord sections stained with hematoxylin/eosin revealed increased inflammation in the *FibγWT* mice versus the *Fibγ390-396A* mice. (D) Survival curve of *Fibγ390-396A* and *FibγWT* mice after MOG_{35-55} immunization. *Fibγ390-396A* had a greater survival rate than the *FibγWT* mice. (E) Rotarod analysis of *Fibγ390-396A* and *FibγWT* mice on day 13. *Fibγ390-396A* significantly outperformed their wild-type counterparts in a behavioral test designed to assess motor skill function. $n = 7$ mice per group. **, $P < 0.05$. (F) Increased activation of $IsoB4^+$ cells in *FibγWT* mice as compared with *Fibγ390-396A* mice. Bar, 58 μm. Data are represented as the mean clinical score and are mean ± SEM.

molecule and is exposed only when fibrinogen is immobilized or converted to fibrin (25, 36). We used 200 μM of peptide, a concentration shown to inhibit adhesion of Mac-1–overexpressing cells to immobilized fibrinogen (37), to examine whether the $\gamma^{377-395}$ peptide could inhibit microglia activation. Fibrinogen treatment resulted in 71 ± 4.9% of activated microglia when compared with 38.3 ± 9.8% after the addition of the $\gamma^{377-395}$ peptide (Fig. 5, A and B; $P < 0.05$), suggesting that the $\gamma^{377-395}$ peptide reduced fibrin-mediated microglia activation. The $\gamma^{377-395}$ peptide did not affect the activation state of untreated microglia and did not inhibit LPS-mediated microglia activation (Fig. 5 B), further suggesting the specificity of $\gamma^{377-395}$ to block the activation of Mac-1 by fibrin. In accordance, examination of Akt phosphorylation showed that the $\gamma^{377-395}$ peptide could specifically inhibit fibrin-mediated and not LPS-mediated phosphorylation of Akt (Fig. 5 C). Overall, these results suggest that inhibition of fibrin–Mac-1 interactions by the $\gamma^{377-395}$ peptide inhibits both the morphological activation and the signaling cascade induced by fibrin-mediated activation of the Mac-1 microglia receptor.

Prophylactic or therapeutic administration of the fibrin $\gamma^{377-395}$ peptide suppresses EAE and inhibits microglia activation in vivo

Because genetic studies showed that the $\gamma^{377-395}$ binding epitope of fibrinogen to Mac-1 is not involved in coagulation (15) but is sufficient to inhibit fibrin-mediated microglia activation (Figs. 4 and 5), we examined whether blocking exclusively the inflammatory properties of fibrinogen in vivo using the $\gamma^{377-395}$ would be sufficient to ameliorate EAE. We therefore examined the effects of in vivo administration of the $\gamma^{377-395}$ fibrin peptide on microglia activation and clinical progression in an animal model for MS. We first assessed the effects of vaccination against $\gamma^{377-395}$ peptide. Vaccination with $\gamma^{377-395}$ peptide before the induction of EAE resulted in a significant reduction in disease penetrance and clinical symptoms. All control mice (15/15) developed clinical symptoms of EAE. In contrast, only 53% of the vaccinated mice (8/15) developed EAE. Moreover, mice vaccinated with the $\gamma^{377-395}$ peptide showed an average clinical score of 1.1, whereas the control group showed a score of 2.5 (Fig. 6 A; $P < 0.01$). In a rotarod test, vaccinated mice showed a 76% increase in motor strength and coordination when compared with the control mice. Quantitative histopathological analysis showed reduced inflammatory lesions in the cerebellum (index of 6.5 ± 5.9 vs. 12 ± 5.2; $P < 0.05$) and spinal cord (index of 1.5 ± 2 vs. 2.3 ± 1; $P < 0.01$) from $\gamma^{377-395}$ peptide–vaccinated mice as compared with control mice.

Because vaccination is a preventive treatment, we further assessed whether $\gamma^{377-395}$ peptide would be beneficial if administered after the onset of disease. We administered intranasally 30 μg $\gamma^{377-395}$ peptide daily after the first paralytic episode in remitting relapsing EAE (35). Intranasal delivery

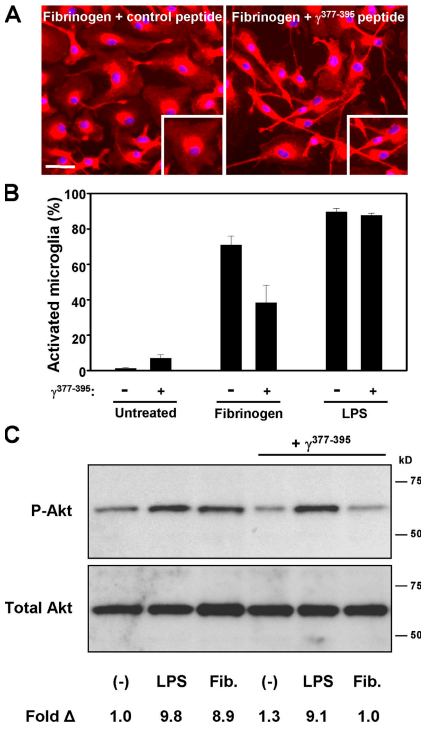

Figure 5. The fibrin-derived $\gamma^{377-395}$ peptide inhibits microglia activation. (A) Microglia activation upon fibrinogen stimulation is attenuated in the presence of $\gamma^{377-395}$. Bar, 33 μm; inset, 29 μm. (B) Quantitation of microglia activation reveals that $\gamma^{377-395}$ diminishes fibrinogen-stimulated microglia activation but has no effect on LPS activation. (C) Treatment of microglia with $\gamma^{377-395}$ blocks fibrinogen-induced Akt activation in vitro. LPS activation of Akt is unaffected by $\gamma^{377-395}$ treatment.

is a noninvasive delivery method that results in a higher degree of drug delivery to the nervous system and a lower degree of systemic drug delivery to tissues such as liver and lymph nodes when compared with intravenous delivery (38). Intranasal delivery has been previously shown to be effective as a method of drug delivery in EAE (39-41). $\gamma^{377-395}$ peptide–treated mice ($n = 14$) compared with control mice ($n = 13$) did not relapse (Fig. 6 B). Peptide-treated mice showed a 1.4-fold increase of motor functions when compared with the control mice after the first relapse on day 29. Administration of scramble peptide had no effect on the progression of EAE (Fig. S5, available at http://www.jem.org/cgi/content/full/jem.20061931/DC1).

Immunohistochemical analysis using Mac-3, a microglia/macrophage marker, revealed reduction of activated cells in the peptide-treated (Fig. 6 D) as compared with control animals (Fig. 6 C). High magnification images of Mac-3 immunostaining are shown in Fig. S6, which is available at http://www.jem.org/cgi/content/full/jem.20061931/DC1. In addition, inducible nitric oxide synthase (iNOS), a major product of activated $CD11b^+$ microglia in EAE (42), was reduced in the $\gamma^{377-395}$ peptide–treated animals (Fig. 6 D, inset). Quantitation of the histopathological analysis shows reduction in both Mac-3 ($P < 0.05$) and iNOS ($P < 0.01$), whereas there are no major differences in T cell infiltrates (Fig. 6 E; $P = 0.48$). We further examined whether the $\gamma^{377-395}$ peptide affected the peripheral immune response. FACS analysis on the splenocytes of mice immunized with $PLP_{139-151}$ using six markers for peripheral immune cells, namely CD4 and CD8 T cells, CD11b macrophages, CD11c dendritic cells, and CD19 and B220 B cells, did not reveal any differences between untreated and $\gamma^{377-395}$ peptide–treated animals (Fig. S4), suggesting that similar to systemic fibrin depletion (Fig. S3), the $\gamma^{377-395}$ peptide does not affect the peripheral immune response. These results are in accordance with prior studies in which depletion of macrophages (43) or microglia (3) resulted in dramatic reduction of clinical symptoms in EAE even in the presence of functional T cells.

The fibrin $\gamma^{377-395}$ peptide does not affect the coagulation properties of fibrinogen

Several studies have demonstrated both in vivo and in vitro that fibrinogen interacts with different cellular receptors via non overlapping epitopes (for review see reference 16). Fibrinogen regulates blood coagulation by engaging the platelet $\alpha_{IIb}\beta_3$ integrin receptor via its $\gamma^{408-411}$ epitope, whereas it mediates inflammatory processes by engaging the Mac-1 receptor via its $\gamma^{377-395}$ epitope. As a result, fibrinogen knock-in mice, where the $\gamma^{390-396}$ Mac-1 binding site has been mutated, show normal coagulation properties, such as platelet aggregation, thrombus formation, and clotting time (15). To determine whether the $\gamma^{377-395}$ peptide interfered with blood coagulation, we examined its effects on the procoagulant properties of fibrinogen both in vivo and in vitro. As expected, the $\gamma^{377-395}$ peptide does not affect coagulation in mice (Fig. 7 A) or prothrombin time (Fig. 7 B). Moreover, in an in vitro fibrin polymerization assay, the $\gamma^{377-395}$ peptide did not alter the polymerization time of fibrin (Fig. 7 C). In contrast, the GPRP peptide, an established inhibitor of clot formation (44), inhibits fibrin polymerization (Fig. 7 C). Collectively, these results show that in vivo delivery of the $\gamma^{377-395}$ peptide reduces the progression and severity of EAE by specifically targeting microglia/macrophage activation in the CNS parenchyma without adverse hemorrhagic effects.

DISCUSSION

In this study, we show for the first time that inhibition of the inflammatory but not the procoagulant properties of fibrinogen is sufficient to suppress clinical symptoms and disease pathogenesis in an animal model of MS. We show that fibrinogen–Mac-1 interaction induces signal transduction pathways that support the activation of microglia and have identified the fibrinogen $\gamma^{377-395}$ polypeptide that contains the Mac-1 binding motif as a therapeutic target for MS. Our study identifies fibrinogen as a microglial activation signal and suggests the following model for the role of fibrin in inflammatory demyelination (also see Fig. 8): (a) Fibrinogen is not present within the extracellular matrix in any normal/unchallenged tissue, including healthy CNS; (b) BBB

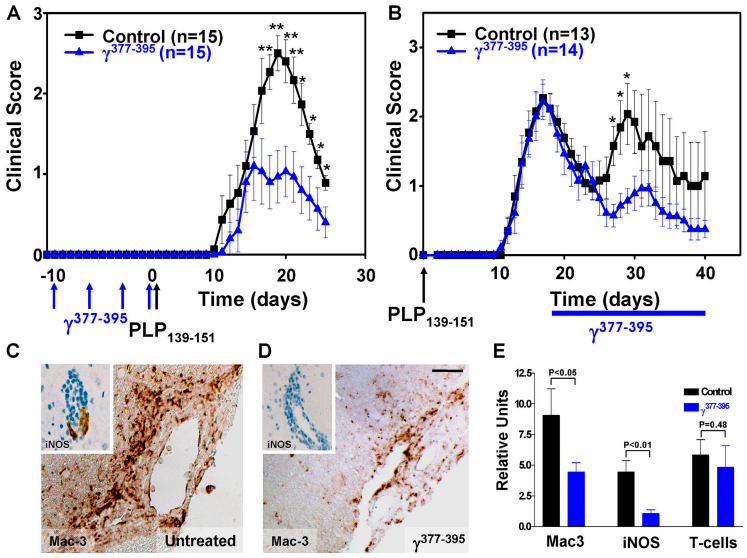

Figure 6. The fibrin-derived $\gamma^{377-395}$ peptide suppresses EAE. (A) Clinical scores from $\gamma^{377-395}$ peptide–vaccinated mice. Mice were immunized with $\gamma^{377-395}$ peptide before EAE induction with $PLP_{139-151}$ peptide. Vaccinated mice (blue triangles; $n = 15$) had significantly reduced clinical scores as compared with control mice (black squares; $n = 15$). (B) Clinical scores from $PLP_{139-151}$–immunized mice where the $\gamma^{377-395}$ peptide was administered every day intranasally after the peak of the initial paralytic episode. $\gamma^{377-395}$–treated mice (blue triangles; $n = 14$) did not show a relapse at approximately day 30 as compared with the controls (black squares; $n = 13$). *, $P < 0.05$; **, $P < 0.01$. Data are represented as the mean clinical score and are mean ± SEM. Immunostaining for Mac-3 and iNOS (inset) on day 30 after immunization shows dramatic reduction of microglia activation in the $\gamma^{377-395}$ peptide–treated mice after EAE induction (D) when compared with control (C). Bar, 20 μm; inset, 10 μm. (E) Quantitation shows a twofold reduction in Mac-3 ($P < 0.05$) and a 4.2-fold reduction in iNOS ($P < 0.01$) after $\gamma^{377-395}$ peptide treatment, whereas there are no major differences in T cell infiltration.

disruption, which precedes lesion development and clinical symptoms in MS (6, 45), permits the leakage of fibrinogen perivascularly in the brain; (c) Fibrinogen is converted to fibrin either by cell-associated procoagulant factors (e.g., tissue factor) expressed within the nervous system or by blood-borne procoagulants (46); (d) Fibrinogen conversion to fibrin allows the exposure of the cryptic Mac-1 binding motif in fibrinogen associated with $\gamma^{377-395}$ sequence (25, 36); (e) Fibrin–Mac-1 interactions induce local activation of microglia, including a fibrin-dependent activation of Akt and Rho signaling, resulting in cytoskeletal rearrangements and increased phagocytic capacity; (f) Fibrin-mediated microglia activation events lead to local degenerative and phagocytic alterations that determine the extent of tissue damage in MS. Therefore, because fibrinogen within the CNS becomes appreciable only after injury or BBB disruption, it could serve as a matrix-associated "danger" signal and support inflammatory processes. Given the colocalization of inflammatory demyelinating lesions in MS with fibrin deposition, our data suggest that fibrinogen–Mac-1 interaction in the CNS parenchyma is central to microglia activation and determines the area of demyelination in MS.

Our study identifies fibrinogen as a ligand for Mac-1 on microglia cells. Complement and in particular iC3b is well established as a ligand for Mac-1 (28). The presence of immunoglobulins and activated complement is restricted to the pattern II MS lesions (1). Because microglia activation and phagocytosis are common features for all subtypes of MS, other factors in the demyelinating lesion could potentially mediate microglia activation. Because BBB disruption is a common feature for different types of MS lesions, our study suggests that fibrin could serve as a broad activation signal for microglia in the CNS. Determination of the temporal and spatial distribution of the different Mac-1 ligands in MS plaques would provide crucial information for the activation of these cells in different disease stages. Activation of microglia contributes to both neuronal (47) and oligodendrocyte death (31) via release of cytokines and nitric oxide. The $\gamma^{377-395}$ peptide induced a reduction of $iNOS^+$ microglia, suggesting that inhibition of fibrin–Mac-1 interaction reduces microglia activation that in MS could mediate secondary damaging effects on other cell types of the nervous system.

Prior studies have shown that genetic ablation of $CD11b^+$ microglia (3) or antibodies against CD11b, such as M1/70 (48), reduce symptoms in EAE. The present studies further underscore the importance of Mac-1 in microglial activation in EAE, but establish that the interaction of Mac-1 with one specific ligand, the provisional matrix protein fibrinogen, is central to the clinical progression of disease and CNS pathologies. A genetic alteration in the endogenous fibrinogen γ chain gene that selectively eliminates the Mac-1 binding motif is sufficient to ameliorate disease pathogenesis in EAE. Interestingly, mutating the Mac-1 binding motif on the fibrinogen γ chain does not affect either the clotting function of fibrinogen or the engagement of Mac-1 with other ligands (15). Consistent with these findings, pharmacologic disruption

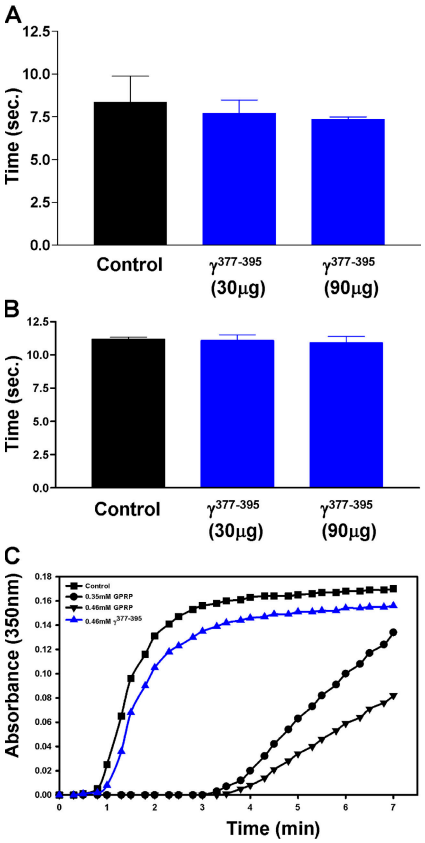

Figure 7. The fibrin-derived $\gamma^{377-395}$ peptide does not affect in vivo coagulation or fibrin polymerization. In vivo clotting time (A) and prothrombin times (B) were assayed in the presence of 30 μg $\gamma^{377-395}$ peptide, the dose administered in vivo daily, and 90 μg $\gamma^{377-395}$ peptide. Neither dose affected blood clotting times. (C) In vitro fibrin polymerization was examined in the presence of the $\gamma^{377-395}$ peptide. GPRP, a known inhibitor of fibrin formation, significantly attenuated fibrin formation, whereas the $\gamma^{377-395}$ peptide had no effect on fibrin polymerization.

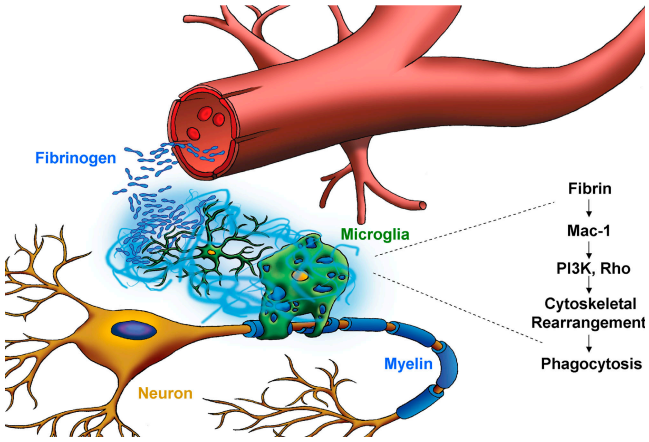

Figure 8. Proposed model for the role of fibrin-induced activation of microglia in inflammatory demyelination. BBB disruption permits the leakage of fibrinogen, the high affinity ligand for Mac-1, in the CNS parenchyma. Fibrinogen is converted to fibrin and functions as the spatial signal to induce local activation of microglia via activation of the Mac-1 integrin receptor and induction of signaling pathways downstream of Mac-1, such as Akt and Rho, resulting in phagocytosis that could determine the extent of tissue damage in inflammatory demyelination.

of fibrinogen–Mac-1 interaction with the fibrinogen-derived blocking $\gamma^{377-395}$ peptide (37) also strongly alleviated CNS disease and did not affect coagulation. For peptide-recognizing integrin receptors, such as the RGD-recognizing αvβ3 and α5β1 integrins, both the peptide itself and antibodies against the peptide may inhibit integrin-mediated biological effects (49-52). Similarly, the $\gamma^{377-395}$ peptide was found not only to directly block fibrinogen–Mac-1–dependent microglial activation events both in vitro (Fig. 5) and in vivo (Fig. 6, B–E), but in addition, vaccination with the $\gamma^{377-395}$ peptide protects from EAE (Fig. 6 A). One inference of this finding is that the generation of monoclonal antibodies against the $\gamma^{377-395}$ epitope could prove valuable therapeutic tools for MS.

Two previous studies have determined that pharmacologically depleting fibrinogen with snake venom–derived protease (ancrod) can prophylactically ameliorate symptoms of EAE (19, 53). In this study, we further demonstrated that administration of ancrod can be beneficial in limiting the clinical manifestations of EAE even after the onset of paralysis (Fig. 3 and Figs. S1 and S2). Although genetic or pharmacological depletion of fibrinogen illustrates the contribution of fibrinogen to inflammatory demyelinating disease, the clinical value of suppression of coagulation with ancrod in the context of a chronic disease such as MS would depend upon the potential adverse hemorrhagic effects. The effective suppression of EAE observed in mice that either express a form of fully clottable fibrinogen that lacks the Mac-1 binding motif or were treated with the $\gamma^{377-395}$ peptide that has no anticoagulatant effects indicates that functional properties of fibrinogen can be therapeutically targeted without necessarily compromising hemostasis. More detailed dose and pharmacological studies focusing on the $\gamma^{377-395}$ peptide or small molecule mimetics will be necessary to reveal the potential effectiveness of this class of inhibitor in the treatment of inflammatory demyelinating disease.

An interesting unresolved question is the importance of the fibrinogen platelet integrin receptor $\alpha_{IIb}\beta_3$ in the progression of MS. Notably, $\alpha_{IIb}\beta_3$ transcripts are present in chronic MS lesions (54), supporting prior evidence for the presence of platelets in inflammatory demyelinating lesions (55). The clinical benefits associated with the mutant form of fibrinogen expressed by Fib$\gamma^{390-396A}$ mice are not likely to be due to any platelet-related process because these mice have been shown to support normal platelet aggregation in vitro and normal platelet thrombus formation in vivo (15). However, the potential contribution of fibrin–$\alpha_{IIb}\beta_3$ interactions in disease pathogenesis in MS could be readily defined in available mice either lacking α_{IIb} or expressing a mutant form of fibrinogen lacking the $\alpha_{IIb}\beta_3$ binding motif.

Fibrin–Mac-1–mediated activation of monocyte cells is well established (17). Therefore, in addition to microglia activation, the $\gamma^{377-395}$ fibrin peptide could inhibit the local

activation and possibly migration of peripheral macrophages in inflammatory demyelination. Our study shows that fibrinogen depletion or treatment with the $\gamma^{377-395}$ peptide attenuates the clinical symptoms in EAE by primarily ameliorating the microglia/macrophage response without interfering with T cell activation. These results are in accordance with previous studies that have established that not only depletion of macrophages (43) or microglia (3) in EAE results in amelioration of clinical symptoms in the presence of functional T cell activation, but also that induction of monocyte and dendritic cell activation can lead to inflammatory demyelination even in the absence of T cells (56). In addition to CD11b, fibrinogen binds to the CD11c chain of the CD11c/CD18 integrin (57). The $\gamma^{377-395}$ fibrin peptide blocks the binding of fibrinogen to both CD11b and CD11c integrins (36). The $CD11c^+$ perivascular dendritic cells are responsible for the presentation of myelin antigens (58, 59). Whether fibrinogen as a ligand for CD11c/CD18 could regulate the cross talk of dendritic cells with T cells in the perivascular space in inflammatory demyelination remains to be resolved. This is of particular interest because recent studies demonstrated that microglia activation regulates leukocyte recruitment (60). Because the $\gamma^{377-395}$ fibrin peptide blocks the binding of fibrin to both CD11b and CD11c integrins, it is possible that targeting the $\gamma^{377-395}$ epitope could diminish the activation of both parenchymal ($CD11b^+$) and dendritic ($CD11c^+$) microglia. More detailed studies will be required to establish whether fibrin affects the cross talk of microglia with cells that are damaged during inflammatory demyelination (61), such as oligodendrocytes and neurons.

Our study has identified the inhibition of fibrin–Mac-1 interactions as a novel strategy for the attenuation of the microglia/macrophage activation in the CNS. Histopathological studies in acute MS have identified perivenous lesions that appear to be driven by activated microglia/macrophages sometimes in the absence of lymphocytes (62, 63). Although the activation of microglia and macrophages plays a central role in the pathogenesis of MS (3, 4, 43, 63), agents that inhibit the microglia/macrophage response have not been developed (64). Although MS is a disease with profound lesion heterogeneity, BBB disruption and microglia activation are common features for the four different subtypes of MS lesions (1). Therefore, targeting fibrin– Mac-1 interactions could be beneficial in different MS subtypes as a microglia-suppressive therapy and could be used in combinational therapies targeting other aspects of MS pathogenesis. In addition to MS, microglia activation is observed in a variety of neurodegenerative diseases characterized by BBB disruption, such as spinal cord injury, stroke, and Alzheimer's disease (16). It is therefore possible that targeting fibrin–Mac-1 interactions could represent a strategy for inhibiting microglia activation in neurodegenerative diseases. Because blocking fibrin–Mac-1 interactions does not interfere with the physiological properties of fibrin in blood coagulation, this strategy could be applied in chronic diseases such as MS without hemorrhagic side effects.

MATERIALS AND METHODS

Animals. 6-wk-old female SJL/J and C57BL/6 mice were purchased from The Jackson Laboratory or Harlan Sprague Dawley. 6-wk-old female $Fib^{\gamma 390-396A}$ mice were generated from double heterozygous matings to produce homozygous $Fib^{\gamma 390-396A}$ mice (15) and $Fib^{\gamma WT}$ littermate mice as controls. $Fib^{\gamma 390-396A}$ mice were backcrossed six generations to C57BL/6 mice (15). All experiments were approved by the University of California, San Diego, Institutional Animal Care and Use Committee.

Induction of EAE. EAE was induced in 6-wk-old female SJL/J or C57BL/6 mice by subcutaneous immunization with 150 μg $PLP_{139-151}$ (HSLGKWLGHPDKF; American Peptide Company and Azco Pharmchem) or 50 μg MOG_{35-55} (MEVGWYRSPFSRVVHLYRDGK; Sigma-Aldrich) in complete Freund's adjuvant (Sigma-Aldrich) supplemented with 200 ng of heat-inactivated mycobacterium tuberculosis H37Ra (Difco Laboratories). Mice were injected intravenously with 200 ng pertussis toxin (Sigma-Aldrich) on days 0 and 2 of the immunization. Mice were scored daily as follows: 0, no symptoms; 1, loss of tail tone; 2, ataxia; 3, hindlimb paralysis; 4, hindlimb and forelimb paralysis; 5, moribund. Data are represented as the mean clinical score and are mean ± SEM, and the Mann-Whitney test was used for statistical analysis. For the survival curve, statistical analysis was performed with the log-rank test using PRISM software.

Systemic defibrinogenation. Mice were depleted of fibrinogen as described previously (65). The pumps deliver 0.5 μl/hour; thus, the mice received 2.4 U ancrod/day. In control animals, buffer-filled mini-pumps were implanted.

Fibrinogen $\gamma^{377-395}$ peptide vaccination. Vaccination was performed as described previously (66) with the following modifications. 5-wk-old female SJL/J mice were immunized with 200 μg fibrinogen $\gamma^{377-395}$ peptide (YSMKETTMKIIPFNRLSIG; Azco Pharmchem) emulsified with an equal volume of incomplete Freund's adjuvant (Sigma-Aldrich). Mice were immunized four times in alternating rear flanks over the course of 2 wk. Control animals were immunized with incomplete Freund's adjuvant.

Intranasal $\gamma^{377-395}$ peptide administration. Fibrinogen $\gamma^{377-395}$ peptide (YSMKETTMKIIPFNRLSIG; Azco Pharmchem) or scramble peptide (KMMISYTFPIERTGLISNK; Azco Pharmchem) was resuspended in 0.9% NaCl at a concentration of 3 mg/ml. Peptides were aliquoted as single doses and stored at −20°C. Mice were administered 5 μl peptide or 0.9% NaCl as a control in each nare daily using a P10 micropipettor (Gilson) beginning after the peak of the first paralytic episode.

Histopathology. Histopathologic analysis and quantitation of inflammation and demyelination in mouse tissue were performed on cryostat or paraffin sections as described previously (67). Sections were stained with hematoxylin/eosin and luxol fast blue/nuclear red. Spinal cord sections were fixed with 2% paraformaldehyde for 10 min at 4°C and immunostained with a sheep anti-fibrinogen antibody (1:200; US Biological), rat anti-CD11b (1:5; Chemicon), von Willebrand Factor (1:1,000; DakoCytomation), iNOS (polyclonal; 1:750; Chemicon), Mac-3 (rat anti–mouse; 1:200; BD Biosciences), and CNPase (monoclonal; 1:2,000; Sternberger Monoclonals). The inflammatory index is defined by the average number of inflammatory blood vessels per spinal cord cross section. 10–15 cross sections per animal were counted by two observers blinded to the genotypes of the mice. For the cerebellum, the number of cuffs was quantified in two cerebellar sections per animal. To additionally analyze the CNS lesions, we counted Luxol Fast Blue/nuclear red–stained sections, and the relative proportions of demyelinated areas (percentage with SEM) were determined using an ocular morphometric grid as described previously (67). For human MS, paraffin-embedded material was obtained from the Archives of the Center for Brain Research, Medical University of Vienna. Double immunofluorescence was performed with antibodies against CD68 and fibrin. Images were collected using an Axioplan 2 Zeiss microscope with an Axiocam HRc camera or were processed for confocal microscopy using Olympus and Zeiss confocal microscopes.

Rotarod behavior test. The rotarod assay was performed on a TSE Rota-Rod apparatus (TSE Technical and Scientific Equipment GmbH) as described previously (68). Rotarod assays were conducted with a 350-s maximum time limit, and means were collected for at least three trials. Statistical calculations were made by using Student's *t* test.

Culture of primary microglia cells. Microglia were isolated from cultures of mixed cortical cells as described previously (69). In brief, cortices from P1 mice were isolated and digested with trypsin (0.4%) for 20 min at 37°C. Cells from four pups were plated onto poly-D-lysine–coated 75 cm^2 tissue culture flasks. The culture medium (DMEM, 10% heat-inactivated FBS, and 1% Pen/Strep) was changed on day 2. After 2–3 wk in culture, the microglia were removed by the addition of 12 mM lidocaine (Sigma-Aldrich) and orbital shaking (180 rpm) for 20 min at 37°C. The cells were centrifuged (350 *g*), and the pellet was resuspended in complete medium and plated onto poly-D-lysine–coated tissue culture dishes. Microglia cell cultures were >95% pure as determined with three different markers, IsoB4, IBA-1, and CD11b. To immobilize fibrinogen, tissue culture dishes were incubated overnight with 50 μg/ml fibrinogen (Calbiochem) in 20 mM Tris, pH 7.5, and 0.1 M NaCl at 37°C for all fibrinogen treatments. To serve as positive controls, LPS (Sigma-Aldrich) was added to the media at 1 μg/ml.

Phagocytosis assay. Phagocytosis assays were performed on both primary murine microglia and a murine microglia cell line (BV2). BV2 cells are an established cell line used to study microglia responses (47). BV2 cells were routinely passaged in DMEM, 20% heat-inactivated FBS, and 1% Pen/Strep. Microglia phagocytosis was assessed using the Vybrant phagocytosis assay kit (Invitrogen) according to the manufacturer's recommendations. Microglia were cultured in 96-well plates at 5,000 cells/well for 36 h at 37°C. Blocking experiments included the addition of 1 μM LY294002 (Cell Signaling), 10 μg/ml rat anti-CD11b (eBioscience), 10 μg/ml rat anti-TLR4 (eBioscience), or 10 μg/ml rat IgG (Jackson ImmunoResearch Laboratories) to the media. Results were obtained from four separate experiments performed in triplicates. Statistical calculations were made by using Student's *t* test.

Morphometry. Primary microglia were used for all morphologic analysis. Cells were plated on coated fibrinogen or in the presence of LPS for 72 h. Microglia were fixed with methanol and immunostained with Isolectin B4 (1:300; Sigma-Aldrich). Blocking experiments involved the daily administration of 10 μg/ml rat anti-CD11b (eBioscience), 10 μg/ml rat IgG (Jackson ImmunoResearch Laboratories), 200 μM $\gamma^{377\text{-}395}$ peptide, or 200 μM of scramble peptide. Results were obtained from six separate experiments performed in duplicates. 250 cells per condition were counted for each individual experiment. Activated microglia were quantitated as those cells >2,000 μm^2. Images were collected using an Axioplan 2 Zeiss microscope with an Axiocam HRc camera and analyzed using the Axiovision 4.5 program (Carl Zeiss). Quantitation of cell area was performed using the Interactive Measurement feature of the Axiovision 4.5 program (Carl Zeiss MicroImaging, Inc.). Statistical calculations were made by using Student's *t* test.

Endotoxin detection assay. Fibrinogen samples were tested for contaminating endotoxins by a Limulus Amebocyte Lysate assay (E-TOXATE kit; Sigma-Aldrich). Fibrinogen-treated samples had undetectable endotoxin levels (<0.5 endotoxin units).

Immunoblots. Western blots were performed using standard protocols (65). Microglia were serum-starved overnight and plated on fibrinogen or with LPS for 6 h. Lysates were electrophoresed on 4–12% gradient SDS-PAGE gels and probed with phospho and total Akt antibodies (1:1,000; Cell Signaling). RhoA activation was performed as described previously (70). In brief, 2×10^7 microglia were plated on fibrinogen for 6 h or with LPS for 10 min. Cell lysates were incubated with GST-Rhotekin agarose beads (provided by J. Heller Brown, University of California, San Diego, San Diego, CA) for 45 min at 4°C. The beads were washed, resuspended in Laemmli sample buffer, and electophoresed on a 15% SDS-PAGE gel. Activated and total Rho were detected with mouse anti-RhoA (1:500; Santa Cruz Biotechnology, Santa Cruz Biotechnology, Inc.). Densitometry was performed using the National Institutes of Health (NIH) Scion Image software using three blots from three separate experiments.

Deconvolution microscopy. Fluorescent images were obtained as described previously (70). Primary microglia were stimulated with fibrinogen as described above. Cells were immunostained with antibodies to total actin (1:100; Sigma-Aldrich) or β-tubulin (1:100; Sigma-Aldrich).

Isolation of mouse splenocytes and T cell proliferation assay. Spleens were removed from control and fibrin-depleted mice after the induction of $PLP_{139\text{-}151}$ EAE and washed in PBS. Spleens were mechanically dissociated with sterile blades and filtered through 70-μm nylon screens. Splenocytes were pelleted and washed with an erythrocyte lysing solution (Biolegend). Cells were washed twice with PBS, counted, and seeded at a density of 0.5×10^6 cells/96 wells. Cells from both control and fibrin-depleted mice were either untreated or stimulated with 20 μg/ml $PLP_{139\text{-}151}$, and proliferation was assayed by BrdU incorporation (Roche Applied Sciences) according to the manufacturer's instructions.

FACS analysis. Primary mouse splenocytes were isolated from control and $\gamma^{377\text{-}395}$ peptide–treated mice immunized with $PLP_{139\text{-}151}$ on day 29 after immunization. Cells were immunostained with antibodies to CD4, CD8, CD11b, CD11c, CD19, and B220 (1:100; Biolegend) and analyzed on a Becton Dickinson FACSCalibur flow cytometer.

Hematological analyses. Citrated plasma was prepared from mice administered intranasally 30 μg or 90 μg $\gamma^{377\text{-}395}$ peptide or saline control daily for 7 d. Plasma clotting times were measured by combining 10 μl of citrated plasma with 10 μl of 2U/ml bovine thrombin (Enzyme Research Laboratories) and 40 mM $CaCl_2$ in a weigh boat floating in a 37°C water bath. Time to clot was determined by mixing with a toothpick. Plasma thrombin times were established as described previously (15). Fibrin polymerization was evaluated by standard turbidity assays using plasma. In brief, citrate plasma (diluted tenfold in 20 mM Hepes, pH 7.4, containing 0.15 M NaCl and 5 mM ε-amino caproic acid) was combined with bovine thrombin (final concentration, 0.2 U/ml; Enzyme Research Laboratories) and Ca^{2+} (10 mM), and OD_{350} measurements were taken every 30 s.

Online supplemental material. Fig. S1 shows low power images of CD11b and fibrinogen double immunofluorescence that demonstrates that fibrin depletion using ancrod decreases microglia activation in EAE. Fig. S2 shows Luxol Fast Blue staining that reveals that fibrin depletion using ancrod reduces demyelinating lesions in EAE. Fig. S3 shows that there is no difference in proliferation under untreated or $PLP_{139\text{-}151}$–stimulated conditions between control and ancrod-treated mice subjected to $PLP_{139\text{-}151}$ EAE. Fig. S4 shows FACS analysis of splenocytes using the markers CD4, CD8, CD11b, CD11c, CD19, and B220 that reveals that the $\gamma^{377\text{-}395}$ peptide has no significant effect on peripheral immune cells compared with control. Fig. S5 shows that a scramble $\gamma^{377\text{-}395}$ peptide has no effect on progression of EAE. Fig. S6 shows high power images of Mac3 immunostaining in the spinal cord of untreated and $\gamma^{377\text{-}395}$ peptide–treated mice after the induction of EAE. The online supplemental material is available at http://www.jem.org/cgi/content/full/jem.20061931/DC1.

We are grateful for the expert technical assistance, support, and advice from James Feramisco and Arrate Mallabiabarrena for deconvolution microscopy at the Moores UCSD Cancer Center Digital Imaging Shared Resource, Brendan Brinkman for confocal microscopy at the UCSD Neuroscience Microscopy Shared Facility, and Joan Heller Brown and Julie Radeff-Huang for the Rho activity assays. We thank Theo Palmer (Stanford University) for providing us with the BV2 microglia cell line. We thank Michael Jardin, Adrienne Andres, and Priscilla Kim for technical assistance. We thank Michael Karin for critical reading of the manuscript.

This investigation was supported in part by a postdoctoral fellowship from the National Multiple Sclerosis Society (NMSS) to R.A. Adams and the NIH/NINDS P30

NS047101 grant to the UCSD Neuroscience Microscopy Shared Facility. This work was supported by the NMSS research grants RG3370 and RG3782, the Wadsworth Foundation Young Investigator Award, the UCSD Academic Senate Grant RE521H, and NIH/NINDS R01 grants NS051470 and NS052189 to K. Akassoglou.

The authors have no conflicting financial interests.

Submitted: 7 September 2006
Accepted: 26 January 2007

REFERENCES

1. Lassmann, H., W. Bruck, and C. Lucchinetti. 2001. Heterogeneity of multiple sclerosis pathogenesis: implications for diagnosis and therapy. *Trends Mol. Med.* 7:115–121.
2. Platten, M., and L. Steinman. 2005. Multiple sclerosis: trapped in deadly glue. *Nat. Med.* 11:252–253.
3. Heppner, F.L., M. Greter, D. Marino, J. Falsig, G. Raivich, N. Hovelmeyer, A. Waisman, T. Rulicke, M. Prinz, J. Priller, et al. 2005. Experimental autoimmune encephalomyelitis repressed by microglial paralysis. *Nat. Med.* 11:146–152.
4. Jack, C., F. Ruffini, A. Bar-Or, and J.P. Antel. 2005. Microglia and multiple sclerosis. *J. Neurosci. Res.* 81:363–373.
5. Minagar, A., and J.S. Alexander. 2003. Blood-brain barrier disruption in multiple sclerosis. *Mult. Scler.* 9:540–549.
6. Kermode, A.G., A.J. Thompson, P. Tofts, D.G. MacManus, B.E. Kendall, D.P. Kingsley, I.F. Moseley, P. Rudge, and W.I. McDonald. 1990. Breakdown of the blood-brain barrier precedes symptoms and other MRI signs of new lesions in multiple sclerosis. Pathogenetic and clinical implications. *Brain.* 113:1477–1489.
7. Nimmerjahn, A., F. Kirchhoff, and F. Helmchen. 2005. Resting microglial cells are highly dynamic surveillants of brain parenchyma in vivo. *Science.* 308:1314–1318.
8. Claudio, L., C.S. Raine, and C.F. Brosnan. 1995. Evidence of persistent blood-brain barrier abnormalities in chronic-progressive multiple sclerosis. *Acta Neuropathol. (Berl.).* 90:228–238.
9. Kwon, E.E., and J.W. Prineas. 1994. Blood-brain barrier abnormalities in longstanding multiple sclerosis lesions. An immunohistochemical study. *J. Neuropathol. Exp. Neurol.* 53:625–636.
10. Wakefield, A.J., L.J. More, J. Difford, and J.E. McLaughlin. 1994. Immunohistochemical study of vascular injury in acute multiple sclerosis. *J. Clin. Pathol.* 47:129–133.
11. Gay, F.W., T.J. Drye, G.W. Dick, and M.M. Esiri. 1997. The application of multifactorial cluster analysis in the staging of plaques in early multiple sclerosis. Identification and characterization of the primary demyelinating lesion. *Brain.* 120:1461–1483.
12. Tang, L., T.P. Ugarova, E.F. Plow, and J.W. Eaton. 1996. Molecular determinants of acute inflammatory responses to biomaterials. *J. Clin. Invest.* 97:1329–1334.
13. Languino, L.R., J. Plescia, A. Duperray, A.A. Brian, E.F. Plow, J.E. Geltosky, and D.C. Altieri. 1993. Fibrinogen mediates leukocyte adhesion to vascular endothelium through an ICAM-1-dependent pathway. *Cell.* 73:1423–1434.
14. Herwald, H., H. Cramer, M. Morgelin, W. Russell, U. Sollenberg, A. Norrby-Teglund, H. Flodgaard, L. Lindbom, and L. Bjorck. 2004. M protein, a classical bacterial virulence determinant, forms complexes with fibrinogen that induce vascular leakage. *Cell.* 116:367–379.
15. Flick, M.J., X. Du, D.P. Witte, M. Jirouskova, D.A. Soloviev, S.J. Busuttil, E.F. Plow, and J.L. Degen. 2004. Leukocyte engagement of fibrin(ogen) via the integrin receptor alphaMbeta2/Mac-1 is critical for host inflammatory response in vivo. *J. Clin. Invest.* 113:1596–1606.
16. Adams, R.A., M. Passino, B.D. Sachs, T. Nuriel, and K. Akassoglou. 2004. Fibrin mechanisms and functions in nervous system pathology. *Mol. Interv.* 4:163–176.
17. Flick, M.J., X. Du, and J.L. Degen. 2004. Fibrin(ogen)-alpha M beta 2 interactions regulate leukocyte function and innate immunity in vivo. *Exp. Biol. Med. (Maywood).* 229:1105–1110.
18. Akassoglou, K., R.A. Adams, J. Bauer, V. Tseveleki, P. Mercado, H. Lassmann, L. Probert, and S. Strickland. 2004. Fibrin depletion decreases inflammation and delays the onset of demyelination in a tumor necrosis factor transgenic mouse model for multiple sclerosis. *Proc. Natl. Acad. Sci. USA.* 101:6698–6703.
19. Paterson, P.Y. 1976. Experimental allergic encephalomyelitis: role of fibrin deposition in immunopathogenesis of inflammation in rats. *Fed. Proc.* 35:2428–2434.
20. Coller, B.S. 1997. Platelet GPIIb/IIIa antagonists: the first anti-integrin receptor therapeutics. *J. Clin. Invest.* 99:1467–1471.
21. Rotshenker, S. 2003. Microglia and macrophage activation and the regulation of complement-receptor-3 (CR3/MAC-1)-mediated myelin phagocytosis in injury and disease. *J. Mol. Neurosci.* 21:65–72.
22. van der Laan, L.J., S.R. Ruuls, K.S. Weber, I.J. Lodder, E.A. Dopp, and C.D. Dijkstra. 1996. Macrophage phagocytosis of myelin in vitro determined by flow cytometry: phagocytosis is mediated by CR3 and induces production of tumor necrosis factor-alpha and nitric oxide. *J. Neuroimmunol.* 70:145–152.
23. Reichert, F., U. Slobodov, C. Makranz, and S. Rotshenker. 2001. Modulation (inhibition and augmentation) of complement receptor-3-mediated myelin phagocytosis. *Neurobiol. Dis.* 8:504–512.
24. Altieri, D.C., R. Bader, P.M. Mannucci, and T.S. Edgington. 1988. Oligospecificity of the cellular adhesion receptor Mac-1 encompasses an inducible recognition specificity for fibrinogen. *J. Cell Biol.* 107: 1893–1900.
25. Lishko, V.K., B. Kudryk, V.P. Yakubenko, V.C. Yee, and T.P. Ugarova. 2002. Regulated unmasking of the cryptic binding site for integrin alpha M beta 2 in the gamma C-domain of fibrinogen. *Biochemistry.* 41:12942–12951.
26. Fenteany, G., and M. Glogauer. 2004. Cytoskeletal remodeling in leukocyte function. *Curr. Opin. Hematol.* 11:15–24.
27. Harrison, R.E., and S. Grinstein. 2002. Phagocytosis and the microtubule cytoskeleton. *Biochem. Cell Biol.* 80:509–515.
28. Ehlers, M.R.W. 2000. CR3: a general purpose adhesion-recognition receptor essential for innate immunity. *Microbes Infect.* 2:289–294.
29. Ugarova, T.P., D.A. Solovjov, L. Zhang, D.I. Loukinov, V.C. Yee, L.V. Medved, and E.F. Plow. 1998. Identification of a novel recognition sequence for integrin alphaM beta2 within the gamma-chain of fibrinogen. *J. Biol. Chem.* 273:22519–22527.
30. Lehnardt, S., L. Massillon, P. Follett, F.E. Jensen, R. Ratan, P.A. Rosenberg, J.J. Volpe, and T. Vartanian. 2003. Activation of innate immunity in the CNS triggers neurodegeneration through a Toll-like receptor 4-dependent pathway. *Proc. Natl. Acad. Sci. USA.* 100: 8514–8519.
31. Lehnardt, S., C. Lachance, S. Patrizi, S. Lefebvre, P.L. Follett, F.E. Jensen, P.A. Rosenberg, J.J. Volpe, and T. Vartanian. 2002. The toll-like receptor TLR4 is necessary for lipopolysaccharide-induced oligodendrocyte injury in the CNS. *J. Neurosci.* 22:2478–2486.
32. Stephens, L., C. Ellson, and P. Hawkins. 2002. Roles of PI3Ks in leukocyte chemotaxis and phagocytosis. *Curr. Opin. Cell Biol.* 14:203–213.
33. Caron, E., and A. Hall. 1998. Identification of two distinct mechanisms of phagocytosis controlled by different Rho GTPases. *Science.* 282:1717–1721.
34. Bell, W.R., S.S. Shapiro, J. Martinez, and H.L. Nossel. 1978. The effects of ancrod, the coagulating enzyme from the venom of Malayan pit viper (A. rhodostoma) on prothrombin and fibrinogen metabolism and fibrinopeptide A release in man. *J. Lab. Clin. Med.* 91:592–604.
35. Youssef, S., O. Stuve, J.C. Patarroyo, P.J. Ruiz, J.L. Radosevich, E.M. Hur, M. Bravo, D.J. Mitchell, R.A. Sobel, L. Steinman, and S.S. Zamvil. 2002. The HMG-CoA reductase inhibitor, atorvastatin, promotes a Th2 bias and reverses paralysis in central nervous system autoimmune disease. *Nature.* 420:78–84.
36. Ugarova, T.P., and V.P. Yakubenko. 2001. Recognition of fibrinogen by leukocyte integrins. *Ann. N. Y. Acad. Sci.* 936:368–385.
37. Ugarova, T.P., V.K. Lishko, N.P. Podolnikova, N. Okumura, S.M. Merkulov, V.P. Yakubenko, V.C. Yee, S.T. Lord, and T.A. Haas. 2003. Sequence gamma 377-395(P2), but not gamma 190-202(P1), is the binding site for the alpha MI-domain of integrin alpha M beta 2 in the gamma C-domain of fibrinogen. *Biochemistry.* 42:9365–9373.
38. Ross, T.M., P.M. Martinez, J.C. Renner, R.G. Thorne, L.R. Hanson, and W.H. Frey II. 2004. Intranasal administration of interferon beta bypasses the blood-brain barrier to target the central nervous system and

cervical lymph nodes: a non-invasive treatment strategy for multiple sclerosis. *J. Neuroimmunol.* 151:66–77.
39. Yura, M., I. Takahashi, S. Terawaki, T. Hiroi, M.N. Kweon, Y. Yuki, and H. Kiyono. 2001. Nasal administration of cholera toxin (CT) suppresses clinical signs of experimental autoimmune encephalomyelitis (EAE). *Vaccine.* 20:134–139.
40. Xiao, B.G., X.F. Bai, G.X. Zhang, and H. Link. 1998. Suppression of acute and protracted-relapsing experimental allergic encephalomyelitis by nasal administration of low-dose IL-10 in rats. *J. Neuroimmunol.* 84:230–237.
41. Ishikawa, M., Y. Jin, H. Guo, H. Link, and B.G. Xiao. 1999. Nasal administration of transforming growth factor-beta1 induces dendritic cells and inhibits protracted-relapsing experimental allergic encephalomyelitis. *Mult. Scler.* 5:184–191.
42. Tran, E.H., H. Hardin-Pouzet, G. Verge, and T. Owens. 1997. Astrocytes and microglia express inducible nitric oxide synthase in mice with experimental allergic encephalomyelitis. *J. Neuroimmunol.* 74:121–129.
43. Brosnan, C.F., M.B. Bornstein, and B.R. Bloom. 1981. The effects of macrophage depletion on the clinical and pathologic expression of experimental allergic encephalomyelitis. *J. Immunol.* 126:614–620.
44. Laudano, A.P., and R.F. Doolittle. 1981. Influence of calcium ion on the binding of fibrin amino terminal peptides to fibrinogen. *Science.* 212:457–459.
45. Vos, C.M., J.J. Geurts, L. Montagne, E.S. van Haastert, L. Bo, P. van der Valk, F. Barkhof, and H.E. de Vries. 2005. Blood-brain barrier alterations in both focal and diffuse abnormalities on postmortem MRI in multiple sclerosis. *Neurobiol. Dis.* 20:953–960.
46. Akassoglou, K., and S. Strickland. 2002. Nervous system pathology: the fibrin perspective. *Biol. Chem.* 383:37–45.
47. Monje, M.L., H. Toda, and T.D. Palmer. 2003. Inflammatory blockade restores adult hippocampal neurogenesis. *Science.* 302:1760–1765.
48. Brocke, S., C. Piercy, L. Steinman, I.L. Weissman, and T. Veromaa. 1999. Antibodies to CD44 and integrin alpha 4, but not L-selectin, prevent central nervous system inflammation and experimental encephalomyelitis by blocking secondary leukocyte recruitment. *Proc. Natl. Acad. Sci. USA.* 96:6896–6901.
49. Meyer, A., J. Auernheimer, A. Modlinger, and H. Kessler. 2006. Targeting RGD recognizing integrins: drug development, biomaterial research, tumor imaging and targeting. *Curr. Pharm. Des.* 12:2723–2747.
50. Ruoslahti, E. 1996. RGD and other recognition sequences for integrins. *Annu. Rev. Cell Dev. Biol.* 12:697–715.
51. Ruoslahti, E., and M.D. Pierschbacher. 1987. New perspectives in cell adhesion: RGD and integrins. *Science.* 238:491–497.
52. Vassilev, T.L., M.D. Kazatchkine, J.P. Van Huyen, M. Mekrache, E. Bonnin, J.C. Mani, C. Lecroubier, D. Korinth, D. Baruch, F. Schriever, and S.V. Kaveri. 1999. Inhibition of cell adhesion by antibodies to Arg-Gly-Asp (RGD) in normal immunoglobulin for therapeutic use (intravenous immunoglobulin, IVIg). *Blood.* 93:3624–3631.
53. Inoue, A., C.S. Koh, K. Shimada, N. Yanagisawa, and K. Yoshimura. 1996. Suppression of cell-transferred experimental autoimmune encephalomyelitis in defibrinated Lewis rats. *J. Neuroimmunol.* 71:131–137.
54. Lock, C., G. Hermans, R. Pedotti, A. Brendolan, E. Schadt, H. Garren, A. Langer-Gould, S. Strober, B. Cannella, J. Allard, et al. 2002. Gene-microarray analysis of multiple sclerosis lesions yields new targets validated in autoimmune encephalomyelitis. *Nat. Med.* 8:500–508.
55. Cross, A.H., and C.S. Raine. 1991. Central nervous system endothelial cell-polymorphonuclear cell interactions during autoimmune demyelination. *Am. J. Pathol.* 139:1401–1409.
56. Furtado, G.C., B. Pina, F. Tacke, S. Gaupp, N. van Rooijen, T.M. Moran, G.J. Randolph, R.M. Ransohoff, S.W. Chensue, C.S. Raine, and S.A. Lira. 2006. A novel model of demyelinating encephalomyelitis induced by monocytes and dendritic cells. *J. Immunol.* 177:6871–6879.
57. Loike, J.D., B. Sodeik, L. Cao, S. Leucona, J.I. Weitz, P.A. Detmers, S.D. Wright, and S.C. Silverstein. 1991. CD11c/CD18 on neutrophils recognizes a domain at the N terminus of the A alpha chain of fibrinogen. *Proc. Natl. Acad. Sci. USA.* 88:1044–1048.
58. McMahon, E.J., S.L. Bailey, C.V. Castenada, H. Waldner, and S.D. Miller. 2005. Epitope spreading initiates in the CNS in two mouse models of multiple sclerosis. *Nat. Med.* 11:335–339.
59. Greter, M., F.L. Heppner, M.P. Lemos, B.M. Odermatt, N. Goebels, T. Laufer, R.J. Noelle, and B. Becher. 2005. Dendritic cells permit immune invasion of the CNS in an animal model of multiple sclerosis. *Nat. Med.* 11:328–334.
60. Zhou, H., B.M. Lapointe, S.R. Clark, L. Zbytnuik, and P. Kubes. 2006. A requirement for microglial TLR4 in leukocyte recruitment into brain in response to lipopolysaccharide. *J. Immunol.* 177:8103–8110.
61. Carson, M.J. 2002. Microglia as liaisons between the immune and central nervous systems: functional implications for multiple sclerosis. *Glia.* 40:218–231.
62. Lucchinetti, C.F., W. Bruck, M. Rodriguez, and H. Lassmann. 1996. Distinct patterns of multiple sclerosis pathology indicates heterogeneity on pathogenesis. *Brain Pathol.* 6:259–274.
63. Barnett, M.H., A.P. Henderson, and J.W. Prineas. 2006. The macrophage in MS: just a scavenger after all? Pathology and pathogenesis of the acute MS lesion. *Mult. Scler.* 12:121–132.
64. Noseworthy, J., D. Miller, and A. Compston. 2006. Disease-modifying treatments in multiple sclerosis. *In* McAlpine's Multiple Sclerosis. G. Ebers, H. Lassmann, B. Matthews, H. Wekerle, and W.I. MacDonald, editors. Churchill Livingstone, Elsevier, Philadelphia. 729–802.
65. Akassoglou, K., W.-M. Yu, P. Akpinar, and S. Strickland. 2002. Fibrin inhibits peripheral nerve regeneration by arresting Schwann cell differentiation. *Neuron.* 33:861–875.
66. Karnezis, T., W. Mandemakers, J.L. McQualter, B. Zheng, P.P. Ho, K.A. Jordan, B.M. Murray, B. Barres, M. Tessier-Lavigne, and C.C. Bernard. 2004. The neurite outgrowth inhibitor Nogo A is involved in autoimmune-mediated demyelination. *Nat. Neurosci.* 7:736–744.
67. Akassoglou, K., J. Bauer, G. Kassiotis, M. Pasparakis, H. Lassmann, G. Kollias, and L. Probert. 1998. Oligodendrocyte apoptosis and primary demyelination induced by local TNF/p55TNF receptor signaling in the central nervous system of transgenic mice: models for multiple sclerosis with primary oligodendrogliopathy. *Am. J. Pathol.* 153:801–813.
68. Akassoglou, K., B. Malester, J. Xu, L. Tessarollo, J. Rosenbluth, and M.V. Chao. 2004. Brain-specific deletion of neuropathy target esterase/swisscheese results in neurodegeneration. *Proc. Natl. Acad. Sci. USA.* 101:5075–5080.
69. Siao, C.J., S.R. Fernandez, and S.E. Tsirka. 2003. Cell type-specific roles for tissue plasminogen activator released by neurons or microglia after excitotoxic injury. *J. Neurosci.* 23:3234–3242.
70. Seasholtz, T.M., J. Radeff-Huang, S.A. Sagi, R. Matteo, J.M. Weems, A.S. Cohen, J.R. Feramisco, and J.H. Brown. 2004. Rho-mediated cytoskeletal rearrangement in response to LPA is functionally antagonized by Rac1 and PIP2. *J. Neurochem.* 91:501–512.